

Article

Quantum Chemical Study of Various Structural TiO₂ Nanoclusters with Photocatalytic Activity

N.Sh. Avazova,¹ J.R. Uzokov¹, A.N. Mukhamadyev¹, N.K. Mukhamadiyev¹.

¹Samarkand state university. Samarkand. Uzbekistan

e-mail: u.javlon03@gmail.com

Abstract: The structural stability of (TiO₂)_n (n=10÷50) nanoclusters with different structures and photocatalytic activity, the position of the reaction centers through the electron density distribution in the molecule, the HUMO and LUMO MO energies, and based on them, the energies and sizes of the lattice gap were calculated using the DFT (B3LYP and CAM-B3LYP) method. According to calculations, the difference (ΔE) between the energy of HUMO and LUMO with increasing number of atoms of the nanocluster (TiO₂)_n (n=10÷50) (DFT) basis set B3LYP/6-31G** is equal to the following values. For n = 5 it was calculated to be 3,5 eV and 2,8 eV for n=20. Bu esa clusterlarda atom sony ortishi bilan tarmog bo'shlyg'ining kamaoesh va photocatalytic faolligi ortishi bildiradi.

Keywords: (TiO₂)_n nanoclusters, DFT, electronic properties, HUMO and LUMO orbitals, band gap, cluster size effects.

Citation: N.Sh. Avazova,¹ J.R. Uzokov², A.N. Mukhamadyev³, N.K. Mukhamadiyev Quantum Chemical Study of Various Structural TiO₂ Nanoclusters with Photocatalytic Activity Central Asian Journal of Medical and Natural Science 2024, 6(1), 81-87.

Received: 10th Oct 2024

Revised: 11th Nov 2024

Accepted: 24th Nov 2024

Published: 30th Nov 2024



Copyright: © 2024 by the authors. Submitted for open access publication under the terms and conditions of the Creative Commons Attribution (CC BY) license (<https://creativecommons.org/licenses/by/4.0/>)

1. Introduction

In recent years, research on the synthesis of semiconductor nanoclusters with photocatalytic activity, their morphology and textural characteristics have increased significantly. Currently, there is increasing attention to the use of promising alternative semiconductor materials rather than traditional methods [1-2]. These processes are cost-effective with relatively simple equipment requirements [3]. Nanomaterials with photocatalytic activity involve the generation of reactive species such as •OH radicals, which enable rapid and efficient oxidation of organic, inorganic, and biological pollutants. Heterogeneous photocatalysis using oxide-based nanomaterials is particularly effective in the removal of water-soluble pollutants from water and wastewater under the influence of light [4].

Titanium dioxide (TiO₂) nanoparticles and composite materials based on them are one of the most promising solutions, unlike others. TiO₂ has attracted much attention due to its important textural characteristics, such as low toxicity, biocompatibility, and wide band gap [5-6]. TiO₂ nanoclusters are a class of nanomaterials with photocatalytic activity due to their high surface area and nanoscale pores. Therefore, TiO₂ clusters serve as an ideal model to study the catalytic properties of nanostructured TiO₂ for pollutant degradation in first-principles calculations. Qu and co-workers [3] The structural and electronic properties of (TiO₂)_n (n=1÷16) nanoclusters were studied as a function of size using first-principles calculations [7]. In these studies, a complete understanding of the

catalytic mechanism of TiO₂ nanoclusters and the first step in the research based on it is to select appropriate structural models with relatively high stability and size. [8]. For example, in 2016, Arab et al. evaluated the structural stability of (TiO₂)_n (n=1÷10) nanoclusters using a first-principles approach by analyzing their energetic properties, including binding energy, second-order energy difference, and dissociation energy [9].

TiO₂ nanoclusters have a hierarchical surface morphology and have been well studied and attracted attention due to their various physicochemical properties that can improve photocatalytic performance. [10]. This strategy has become one of the excellent ways to solve problems related to the kinetic and thermodynamic aspects of TiO₂ photocatalyst [11]. The hierarchical nanostructure design for TiO₂ resulted in better molecular diffusion kinetics, improved absorption of incident light, increased surface area, and excellent charge carrier separation with less chance of recombination.

There are different phases of TiO₂, among which the most stable and common form is rutile. Rutile occurs naturally and is used in industry in photocatalytic applications where activation by sunlight is not required. It has high optical and mechanical density. The anatase phase of TiO₂ has stronger photocatalytic properties than rutile, so it is widely used in photocatalytic and self-cleaning coatings that work under sunlight. Anatase is more commonly used in fine fibers and thin coatings. Anatase is the phase with the highest photocatalytic activity, the wide band gap value of both phases (3,0-3,2 eV) leads to the activation of these materials under UV-VIS light irradiation. [12]. To make the photocatalysis process sustainable, it is necessary to develop materials that are highly photoreactive under sunlight. Considering that sunlight contains only 4-5% of UV-VIS rays, the need to find nanostructures with visible light absorption that accounts for 50% of the solar spectrum becomes necessary [13]. Numerous nanoscale modifications of TiO₂ have been performed to achieve complete photoactivation of this semiconductor under visible light irradiation. Composites obtained with non-metallic compounds have yielded partially positive results, since the red shift of the absorption edge of TiO₂, in turn, increases the recombination rate of the hole-electron pair. The creation of heterostructures based on TiO₂ combined with low-bandgap semiconductors may be an effective approach to improve the photocatalytic conversion of pollutants in water [13]. The fundamentals of the synthesis and photoactivation of TiO₂ low-bandgap semiconductor heterostructures are explored, and some of the data on the photocatalytic activity of these materials are presented to shed light on the potential of their use for water purification. on a large scale.

2. Materials and Methods

Quantum chemical calculations were performed on the stable structure of (TiO₂)_n (n=10÷50) nanoclusters. Calculation of the charge density distribution in the molecule for the optimized structure of the nanoclusters was performed using the semi-empirical (PM3), electrostatic potential, reactivity descriptors, and values of the stable energies using the density functional theory (DFT) Monte Carlo algorithm and the B3LYP/6-31G** basis set [14-15]. For easy access to the calculations of molecular orbital energies, the values of the HOMO and LUMO levels were obtained.

3. Results and discussions

Quantum chemical calculations, including BLYP, B3LYP, and CAM-B3LYP DFT calculations, were performed on various optimized geometric structures of TiO₂ nanoclusters (Figure 1).

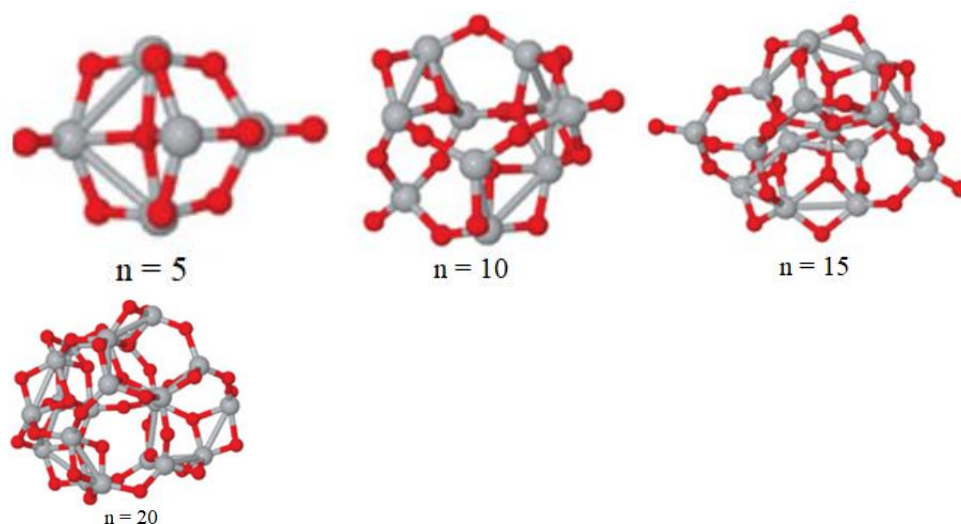


Figure 1. Optimized geometric structure of $(\text{TiO}_2)_n$ nanoclusters

Using the LANL2DZ basis set and semi-empirical PM3 methods, the calculated results show that the Ti-O bond lengths vary very little with increasing number of atoms in the clusters. In particular, the length of the Ti-O bonds in the $n = 5$ cluster was calculated to be $1,864 \text{ \AA}$, $1,848 \text{ \AA}$ for $n = 10$, around $1,836 \text{ \AA}$ for $n = 15$, and $1,832 \text{ \AA}$ for $n = 20$ Ti-O bonds. From this it can be concluded that the stability of clusters increases with increasing number of atoms.

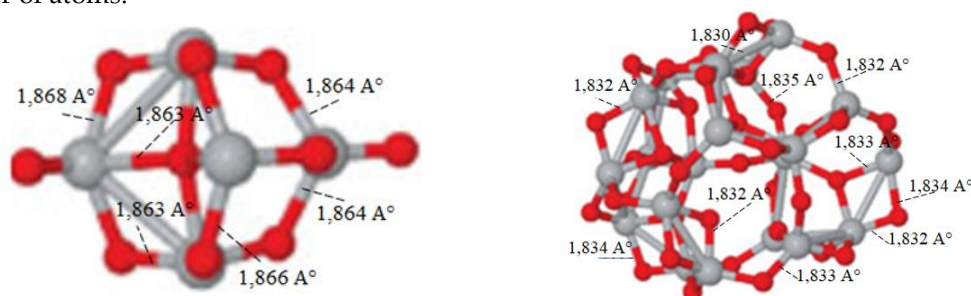


Figure 2. The length of Ti-O bonds in the $(\text{TiO}_2)_n$ ($n = 5$ and 20) cluster

The vibrational binding energies of clusters with different structures were calculated (DFT) using the optimized geometry of the clusters using the B3LYP/6-31G** basis set. For clusters with $n \leq 15$, the singlet and triplet states are close to each other. It was observed that as the number of atoms in the clusters increased, the binding energies of the singlet-state bound atoms became higher than those in the triplet-state. This once again confirms that the stability of the clusters increases with the number of atoms in the clusters. Quantum chemical analysis of $(\text{TiO}_2)_n$ ($n=5, 10, 15, 20$) nanoclusters shows that the structural and electronic properties vary significantly depending on the cluster size. Larger clusters exhibit enhanced stability and reduced chemical reactivity due to changes in the total energy and band gap energy. These trends indicate that $(\text{TiO}_2)_n$ clusters, especially those with high atomic sizes, are of interest for practical applications requiring stable and conductive nanomaterials. The most important physical parameters of the clusters, obtained based on (DFT) B3LYP/6-31G** calculations, are listed in Table 1.

Table 1.

Some physical parameters of $(\text{TiO}_2)_n$ ($n = 5 \div 20$) clusters

$(\text{TiO}_2)_n$	Total energy E, (eV)	Chemical potential (eV)	Electrophilic index (eV)	Dipole moment (Debye)
5	-235,5	-3,2	1,5	4,3
10	-477,3	-2,9	1,7	4,7

15	-716,5	-2,7	1,8	5,1
20	-957,1	2,5	2,0	5,4

In large clusters, the total energy is energy, which seems to improve the quality of the case. It helps such products to remain active for a long time in photocatalytic processes.

The Hirshfeld surface image (density surface) of the $(\text{TiO}_2)_n$ cluster was studied using the Cristal Explorer 17 software. The Hirshfeld surface image provides an effective representation of the electron density and charge distribution. Image analysis is important for studying the electron distribution and polarization of clusters (Figure 3). The colors obtained from the surface analysis indicate the polarization on the surface. Green color indicates areas with neutral charge on the surface, yellow and red colors indicate areas with high electron density or partially negatively charged parts. Blue indicates areas with low electron density. It can be seen that the green color dominates in the 3D image obtained from the Hirshfeld surface analysis. This indicates that the charge distribution in the $(\text{TiO}_2)_5$ cluster is almost the same. The red and yellow colors indicate the magnitude of the electron density concentrated around the electronegative element oxygen atom in the cluster (Figure 3a).

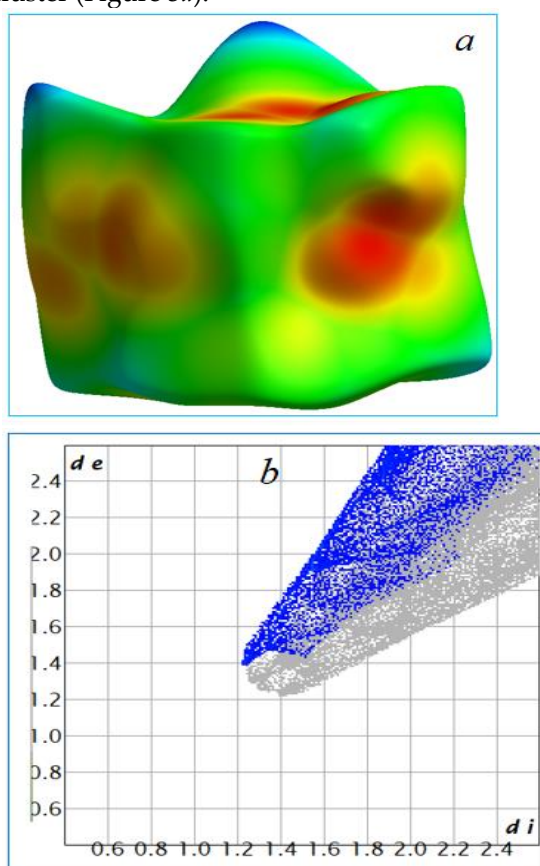


Figure 3. Hirshfeld surface image (a) and Hirshfeld fingerprints (b) of a $(\text{TiO}_2)_5$ cluster

The blue regions in the Hirshfeld fingerprint plot represent strong dipole-dipole interactions. These regions are located on the surface of the cluster, indicating that the main interactions are stronger at these points. These strong interactions can form between oxygen atoms and titanium atoms because oxygen is the more electronegative element, attracting electrons and significantly affecting the charge distribution. The gray dots typically represent weaker interactions, or Van der Waals forces. These forces do not form strong bonds, but they help stabilize the cluster structure. The dense arrangement of gray dots indicates that there are large areas in the cluster that are bound by weak interactions.

As the number of atoms increases, the photocatalytic activity of $(\text{TiO}_2)_n$ nanoclusters also increases, meaning that larger clusters are more efficient in photocatalytic processes

than smaller ones. The main reasons for this are: first, increased energetic stability. Clusters with many atoms have a higher total energy value, which helps them remain active in photocatalytic processes for a longer time. Second, decreased band gap energy: As the number of atoms increases, the band gap energy also changes. This is important for photocatalysis, because when the number of atoms is small, the clusters can absorb more visible light. Increasing the light energy increases the photocatalytic activity and the process. HOMO and LUMO Energy (Figure 4). The distance between the HUMO (Highest Occupied Molecular Orbital) and LUMO (Lowest Unoccupied Molecular Orbital) energies decreases with increasing cluster size (n). This energy difference is called the band gap or band gap, and it is expressed in electron volts (eV) rather than in units of size (nm).

The energetic and structural properties of a cluster are related to its band gap (forbidden region). If the forbidden region is small, that is, the distance between the HOMO and LUMO energy levels is small, then this cluster can absorb low-energy (long-wave) radiation. This allows it to absorb more radiation in the solar spectrum, that is, the photocatalytic activity increases (Figure 5). As the forbidden region becomes smaller, the cluster has a higher photocatalytic activity and is able to effectively decompose organic pollutants in water (for example, dyes such as methylene blue). This is possible precisely due to the red and yellow electron density regions observed on the Hershfeld surface.

In $(\text{TiO}_2)_n$ clusters, when the atomic number increases from 5 to 20, the band gap energy and its size (wavelength) change in the following ranges in the (DFT) B3LYP/6-31G** basis set as follows. For $n = 5$, the band gap energy decreases to 3,5 eV, and when $n = 20$, the band gap energy decreases to 2,8 eV. The wavelength corresponding to the band gap energy is calculated using the Planck constant and the speed of light:

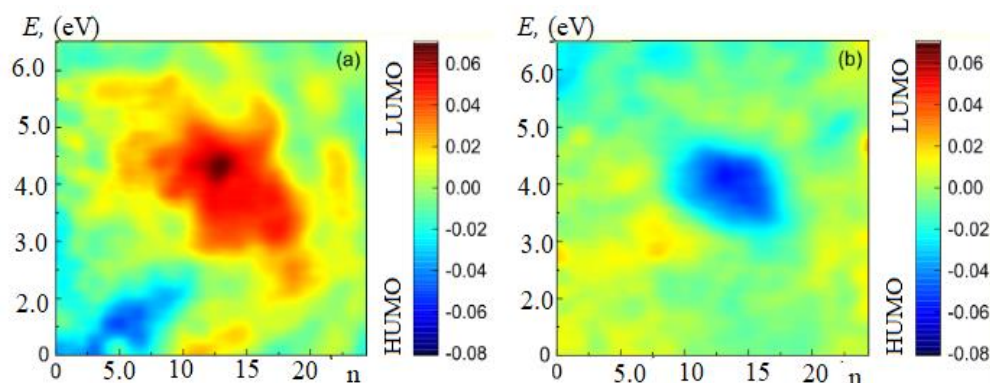


Figure 4. The lattice gap energy of $(\text{TiO}_2)_n$ clusters

These figures suggest that as clusters grow in size, their light absorption spectrum broadens and they can more effectively absorb low-energy (longer wavelength) radiation. Therefore, larger clusters are more efficient in photocatalytic processes involving sunlight.

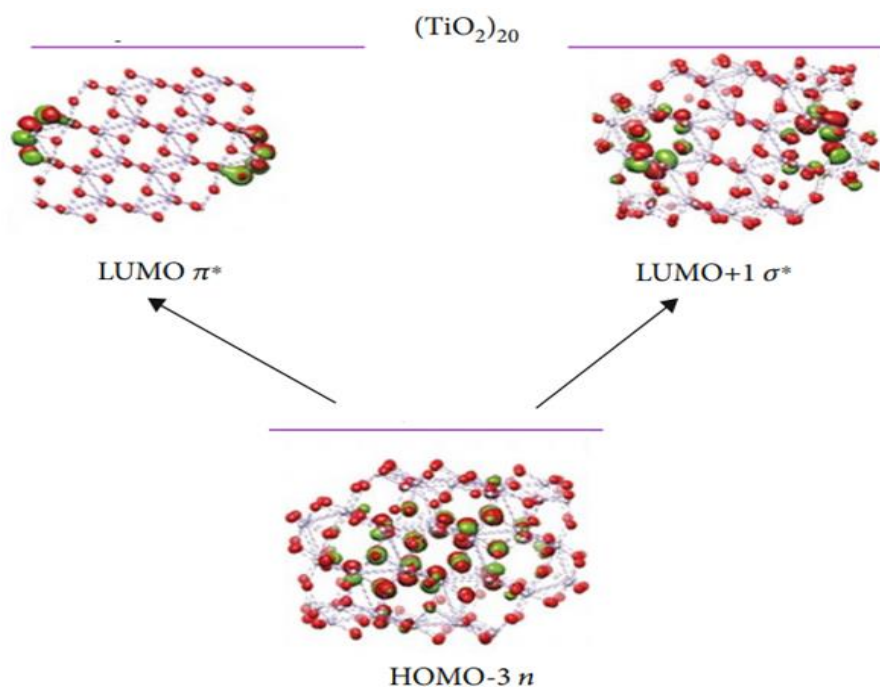


Figure 5. (HUMO and LUMO molecular orbitals of the $(\text{TiO}_2)_{20}$ cluster

Based on data obtained from quantum chemical calculations, it can be concluded that with increasing atomic number, the band gap energy of clusters decreases and their stability increases, which further increases their photocatalytic activity.

4. Conclusion

1. Quantum chemical calculations were performed on the stable structure of $(\text{TiO}_2)_n$ ($n=10-50$) nanoclusters with optimized different geometric structures based on B3LYP and CAM-B3LYP DFT.

2. According to the calculated results, it was found that the length of Ti-O bonds changes with the increase in the number of atoms in the clusters. In the $n = 5$ cluster, the length of Ti-O bonds is calculated to be $1,864 \text{ \AA}$, for $n = 10$ it is $1,848 \text{ \AA}$, for $n = 15$ it is around $1,836 \text{ \AA}$, and for $n = 20$ the length of Ti-O bonds is $1,832 \text{ \AA}$. From this it can be concluded that the stability of the clusters increases with the increase in the number of atoms. Klasterlarda $(\text{TiO}_2)_n$ klasterining $n=5$ dan $n=20$ o'lganda Umumiy energiya E , (eV) ranged from $-235,5 \text{ eV}$ to $-957,1 \text{ eV}$, indicating that large clusters are relatively stable.

3. When the atomic number in $(\text{TiO}_2)_n$ clusters increases from 5 to 20, the energy of the forbidden region (lattice gap) and its size (wavelength) change are found to be equal to the following values in the (DFT) B3LYP/6-31G** basis set. For $n = 5$, the forbidden region energy is calculated to be $3,5 \text{ eV}$, and for $n = 20$, it is found to be equal to 3.5 eV . This indicates that with the increase in the atomic number in the clusters, the lattice gap decreases and the photocatalytic activity increases.

REFERENCES

1. Satoh, N. T., Nakashima, K., & Kamikura, K. (2008). *Nature Nanotechnology*, 3(1), 106-111.
2. Wahlström, E. (2003). Bonding of gold nanoclusters to oxygen vacancies on rutile TiO_2 (110). *Physical Review Letters*, 90(2), 026101.
3. Le Bahers, T., Rerat, M., & Sautet, P. (2014). Semiconductors used in photovoltaic and photocatalytic devices: Assessing fundamental properties from DFT. *The Journal of Physical Chemistry C*, 118(12), 5997-6008.

4. Kullgren, J., et al. (2010). B3LYP calculations of cerium oxides. *The Journal of Chemical Physics*, 132(5).
5. Stephens, P. J., Devlin, F. J., Chabalowsky, C. F., & Frisch, M. J. (1994). Ab initio calculation of vibrational absorption and circular dichroism spectra using density functional force fields. *The Journal of Chemical Physics*, 98(45), 11623–11627. <https://doi.org/10.1021/j100096a001>
6. Cheng, J., et al. (2012). Hole localization and thermochemistry of oxidative dehydrogenation of aqueous rutile TiO₂ (110). *ChemCatChem*, 4(5), 636-640.
7. Wang, Y. (2006). DFT study of solvent effects for some organic molecules using a polarizable continuum model. *Journal of Solution Chemistry*, 35, 869-878.
8. Persson, P., et al. (2006). Quantum chemical calculations of the influence of anchor-cum-spacer groups on femtosecond electron transfer times in dye-sensitized semiconductor nanocrystals. *Journal of Chemical Theory and Computation*, 2(2), 441-451.
9. Arzimurodova, X., Ismatov, D. M., Uzokov, J. R., Mukhamadiyev, A. N., & Mukhamadiev, N. Q. (2022). Quantum chemical evaluation of complex formation of Co (II) ions with quercetin molecule. *Central Asian Journal of Medical and Natural Science*, 3(3), 338-344.
10. Usmonova, H., Uzokov, J. R., Mukhamadiev, N. Q., & Mukhamadiev, A. N. (2022). Study of structural and electronic properties of (ZnO)_n (n = 10–30) nanoclusters using quantum chemical methods. *Central Asian Journal of Medical and Natural Science*, 3(6), 428-434.
11. Xodjayova, G., Ergashev, S., Uzokov, J., & Boboyorova, N. (2024). Quantum chemical study of the synthesis of a chlato complex based on Ni (II) cation and 1,3,5-tris-(beta oxoethyl) hexahydroxo-s-triazine. *Science and Innovation*, 3(A3), 75-82.
12. Saravanan, R., et al. (2011). ZnO/CdO composite nanorods for photocatalytic degradation of methylene blue under visible light. *Materials Chemistry and Physics*, 125(1-2), 277-280.
13. Mazheika, A. S., Matulis, V. E., & Ivashkevich, O. A. (2010). Quantum chemical study of adsorption of Ag₂, Ag₄, and Ag₈ on stoichiometric TiO₂ (110) surface. *Journal of Molecular Structure: Theochem*, 942(1-3), 47-54.
14. Garrity, K. F., et al. (2014). Pseudopotentials for high-throughput DFT calculations. *Computational Materials Science*, 81, 446-452.
15. Kılıç, M., & Çınar, Z. (2009). A quantum mechanical approach to TiO₂ photocatalysis. *Journal of Advanced Oxidation Technologies*, 12(1), 37-46.
16. Ciofini, I., & Daul, C. A. (2003). DFT calculations of molecular magnetic properties of coordination compounds. *Coordination Chemistry Reviews*, 238, 187-209.
17. Bognár, S. (2024). Advancing wastewater treatment: A comparative study of photocatalysis, sonophotolysis, and sonophotocatalysis for organics removal. *Processes*, 12(6), 1256.
18. Jourshabani, M. (2024). Nitrogen-doped carbon quantum dot as electron acceptor anchored on graphitic carbon nitride nanosheet for improving rhodamine B degradation. *Materials Science and Engineering: B*, 305, 117417.
19. Fonseca Guerra, C., et al. (1998). Towards an order-N DFT method. *Theoretical Chemistry Accounts*, 99, 391-403.
20. Ahmed, M. T. (2024). The adsorption of CO gas on the surface of boron nitride incorporating 2D carbon allotropes: A DFT analysis. *Physica Scripta*, 99(6), 0659.